

Role of calcium in phototoxicity of 2-butylamino-2-demethoxy-hypocrellin A to human gastric cancer MGC-803 cells

Zhixiang Zhou, Hongying Yang, Zhiyi Zhang*

Center for Molecular Biology, Institute of Biophysics, Chinese Academy of Sciences, 15 Datun Road, Chaoyang District, Beijing 100101, PR China

Received 14 June 2002; received in revised form 22 October 2002; accepted 13 November 2002

Abstract

After incubation with 2-butylamino-2-demethoxy-hypocrellin A (2-BA-2-DMHA), photodynamically induced change in the cytoplasmic free calcium concentration ($[Ca^{2+}]_i$) and its effect on cell damage were investigated in human gastric cancer (MGC-803). Fluorescence spectrophotometry measurement indicated that the photosensitization of MGC-803 by 2-BA-2-DMHA caused an increase in intracellular calcium $[Ca^{2+}]_i$, and this increase in $[Ca^{2+}]_i$ showed a dependence on the concentration of 2-BA-2-DMHA, light dose and extracellular $[Ca^{2+}]_e$. This phenomenon of intracellular calcium accumulation was further confirmed by using laser scanning confocal microscopy (LSCM). Furthermore, the results from MTT assay and flow cytometry analysis suggested that chelation of extracellular calcium by EGTA or intracellular calcium by BAPTA could inhibit photodynamically induced cell killing, while increase of $[Ca^{2+}]_i$ by thapsigargin (TG), a highly specific inhibitor of the Ca^{2+} -ATPase, or by A23187, a calcium ionophore could enhance this action. Meanwhile, the nucleus morphology was also investigated by fluorescence microscopy. The results indicated that the increase in intracellular Ca^{2+} concentration was responsible for 2-BA-2-DMHA photodynamically induced damage to MGC-803.

© 2002 Elsevier Science B.V. All rights reserved.

Keywords: 2-butylamino-2-demethoxy-hypocrellin A (2-BA-2-DMHA); Human gastric cancer (MGC-803); Photodynamic treatment (PDT); Intracellular calcium $[Ca^{2+}]_i$; Extracellular calcium $[Ca^{2+}]_e$.

1. Introduction

As the most important intracellular signal, molecular calcium is involved in the regulation of several cellular processes in vitro and in vivo experimental systems [1–4]. In resting cells, the cytosolic free Ca^{2+} concentration $[Ca^{2+}]_i$ is buffered to about 100–200 nM by cellular Ca^{2+} buffers and membrane-bound Ca^{2+} transport systems. However, on stimulation, $[Ca^{2+}]_i$ can increase rapidly before being returned to resting levels [4–7].

Recent studies have shown that disruption of intracellular calcium homeostasis has been associated with pathological and toxicological processes [2,6–9]. There is evidence that photodynamic treatment (PDT) of cells is accompanied by an increase in $[Ca^{2+}]_i$ [6,10,11], which may eventually lead

to cell death [12,13], a fact that is of particular interest in tumor therapy.

Gastric cancer, a highly important malignancy, is one of the most common human solid tumors around the world [14], and PDT has been applied to the treatment of gastric tumors in China since 1982 [15] and in Japan since 1980 [16] and has been proven to have great potential. Therefore, knowledge about the phototoxic mechanism in gastric cancer cells is of interest. We have previously reported that treatment of human gastric adenocarcinoma MGC-803 cells with a novel photosensitizer, 2-butylamino-2-demethoxy-hypocrellin A (2-BA-2-DMHA) and red light induced the cells to undergo apoptosis [17], and showed that photosensitivity of MGC-803 cell is increased by decreasing Bcl-2 expression [18] and overexpression of wild-type p53 genes in cells [19]. Here, the aim of this study is to clarify changes in intracellular Ca^{2+} concentrations in cultured MGC-803 cells during photodynamical treatment by 2-BA-2-DMHA, and describes whether calcium plays a role in the photodynamic damage process.

* Corresponding author. Tel.: +86-10-6488-8571; fax: +86-10-6487-1293.

E-mail address: zhangzhy@sun5.ibp.ac.cn (Z. Zhang).

2. Materials and methods

2.1. Chemicals

We have previously synthesized and purified 2-BA-2-DMHA as reported [17], and the purity assessed by high-performance liquid chromatography was higher than 95%. For the *in vitro* cellular experiments, the photosensitizer was dissolved in DMSO at 2.0 mM and stored at -20°C in the dark. Immediately before use, it was diluted with culture medium to desired concentrations. The final concentration of DMSO did not exceed 1% (v/v). The photosensitizer and cells incubated with photosensitizer were protected from light at all times except for the time of planned exposure.

RPMI-1640 medium and fetal bovine serum (FBS) were purchased from GIBCO-BRL (Grand Island, NY, USA). The membrane-permeable Ca^{2+} indicators Fura-2/AM and Fluo-3/AM were obtained from Molecular Probes (Eugene, OR, USA). 3-(4,5-di-methylthiazolyl-2)-2,5-diphenyl-2H-tetrazolium bromide (MTT) and propidium iodide (PI) were from Sigma Chemical Co. (St. Louis, MO, USA). EGTA, BAPTA/Am, TG, A23187 and Hoechst dye 33258 (HO258) were purchased from Molecular Probes. Other reagents were of analytical grade.

2.2. Cell culture

Human gastric adenocarcinoma MGC-803 cells were cultured in RPMI-1640 medium containing 7.5% FBS and antibiotics PS (80 U ml^{-1} penicillin and 100 $\mu\text{g ml}^{-1}$ streptomycin) at 37°C in a humidified atmosphere of 95% air and 5% CO_2 . The cells were maintained in exponential growth in monolayer cultures.

2.3. Cell treatment with 2-BA-2-DMHA and irradiation

Exponentially growing MGC-803 cells in 75 cm^2 flasks were incubated with 2-BA-2-DMHA in RPMI-1640 medium (FBS-free) for 4 h at 37°C in the dark. Then the cells were detached using 0.25% trypsin solution in phosphate-buffered saline (PBS) and collected for use in the following experiment.

The light source was a Red Light Treatment Instrument (Institute of Electronics, Academia Sinica, China). Its total power output was 50 mW cm^{-2} at the position of the samples as measured with a BTY-8204 radiometer (Beijing Institute of Solar Energy, China). Its major emission was more than 90% at 600–700 nm.

2.4. Intracellular calcium measurements

After incubation with 2-BA-2-DMHA in RPMI-1640 medium (FBS-free) for 4 h at 37°C in the dark, cells were collected, washed and loaded with 2 μM Fura-2/AM for another 30 min in oxygenated (95% O_2 , 5% CO_2) Krebs

solution (118.5 mM NaCl, 4.7 mM KCl, 1.2 mM KH_2PO_4 , 1.8 mM CaCl_2 , 1.2 mM MgSO_4 , 10 mM glucose and 25 mM NaHCO_3 , pH 7.4) [20]. Then the cells were gently washed twice with Krebs solution, and suspended in Krebs solution (without Mg^{2+}) [21] at a concentration of 10^6 cells ml^{-1} . Fluorescence emission was measured using Hitachi-4500 fluorescence spectrophotometer in a quartz cuvette equipped with a magnetic stirrer bar. After subtracting background fluorescence caused by cells, the $[\text{Ca}^{2+}]_i$ was calculated by measuring the fluorescence intensity (510 nm emission) with excitation at 340 and 380 nm as described by Gryniewicz et al. [22] and according to the following equation:

$$[\text{Ca}^{2+}]_i = K_d(F_0/F_s)(R - R_{\min})/(R_{\max} - R)$$

where K_d is 225 nM, R the ratio 340:380 of fluorescence of the Fura-2, R_{\min} the ratio 340:380 of Fura-2 in Ca^{2+} -free solution, R_{\max} the ratio of Fura-2 in the presence of saturating Ca^{2+} concentration (1 mM CaCl_2) and F_0/F_s the ratio of 380 nm excitation fluorescence at zero (by adding 5 mM EGTA) and saturating Ca^{2+} (by adding 10% Triton X-100) levels.

2.5. LSCM detection of intracellular calcium distribution in individual cells during PDT

MGC-803 cells cultured in sterile dishes with coverslips for 12 h were treated with 2-BA-2-DMHA for 4 h and then washed and stained with 10 $\mu\text{g ml}^{-1}$ Fluo-3/AM for another 30 min, then gently washed with Krebs solution. After that, fresh Ca^{2+} medium or Ca^{2+} -free medium was filled again. The concentration changes of intracellular Ca^{2+} in arbitrary single cells were monitored by laser confocal scanning microscopy (LSCM Leica, TCS-SP2 type, Germany) at 488 nm excitation wavelength. The Ca^{2+} fluorescence intensity and distribution were analyzed using image analysis software (Leica TCS SP2, Ver. 1.6.582) of Leica Confocal Microscope Systems (Leica Co., Germany).

2.6. Cell survival studies

Ethylene glycol-bis (β -aminoethyl ether) N,N,N,N -tetraacetic acid (EGTA), a known extracellular calcium chelator, and 1,2-bis (2-aminophenoxy)-ethane- N,N,N,N -tetraacetic acid (BAPTA), an intracellular calcium chelator, were used to chelate the extracellular and intracellular calcium, respectively. Thapsigargin (TG), a highly specific inhibitor of the ER-associated Ca^{2+} pump, and Br-A23187, a calcium ionophore, were used in this study to deplete intracellular Ca^{2+} pool and then increase the $[\text{Ca}^{2+}]_i$. Thus, the effects of $[\text{Ca}^{2+}]_i$ and $[\text{Ca}^{2+}]_e$ on the cell survival were quantified by measuring dehydrogenase activity retained in the cultured cells, using MTT assay [23,24]. With a further 30 min incubation in darkness after being treated by PDT

with different Ca^{2+} level conditions, cells were separated and transferred into flat-bottomed 96-well plates (Nunc, Denmark), 100 μl in each well containing 3×10^4 cells in culture medium and then incubated at 37 °C in a CO_2 incubator for 20 h. Viability was determined by adding 50 μl MTT (1 mg ml^{-1} in PBS) to each well and the mixture was incubated for another 4 h at 37 °C. Then culture medium was replaced with 150 μl DMSO to stop MTT reduction and to dissolve the blue formazan crystals produced by mitochondrial hydrogenases in living cells. The plates were shaken at room temperature for 30 min and read immediately at 595 nm on a Bio-Rad model 3550 microplate reader (Richmond, CA, USA). Samples were measured in 12 replicates and each experiment was repeated at least twice. Survival of PDT-treated cells was normalized against cells incubated with photosensitizer alone.

2.7. Flow cytometric detection of DNA fragmentation

For flow cytometric analysis after PDT treatment with the same conditions as shown in Section 2.6, 1×10^6 cells were harvested and washed gently three times with cold

PBS, and then fixed in 70% ethanol at 4 °C for 24 h. Cells were washed twice with PBS and suspended in PBS with RNase A (100 mg ml^{-1}) and incubated at 37 °C for 30 min. At this point, cells were stained with 50 μl ml^{-1} propidium iodide at room temperature for another 30 min at 4 °C, then filtered through a nylon mesh filter. To determine the number of DNA fragments, the specimens were applied to an Epics XL flow cytometer (Coulter, USA). Results were expressed as the percentage of cells exhibiting subdiploid ($<2N$) amounts of DNA relative to the total number of cells analyzed.

2.8. Nuclear morphology in single apoptotic MGC-803 cell using fluorescence microscope

Cells growing on glass were treated with the same conditions as Section 2.6, then treated and control cells were incubated in RPMI-1640 with 7.5% FBS for 20 h at 37 °C in the dark. After that, Hoechst 33258 at final concentrations of 10 μl ml^{-1} , was added to the culture medium and incubated for another 30 min. The cells were then gently washed three times with PBS. The fluorescence image of nuclear morphology in a single cell was monitored using a

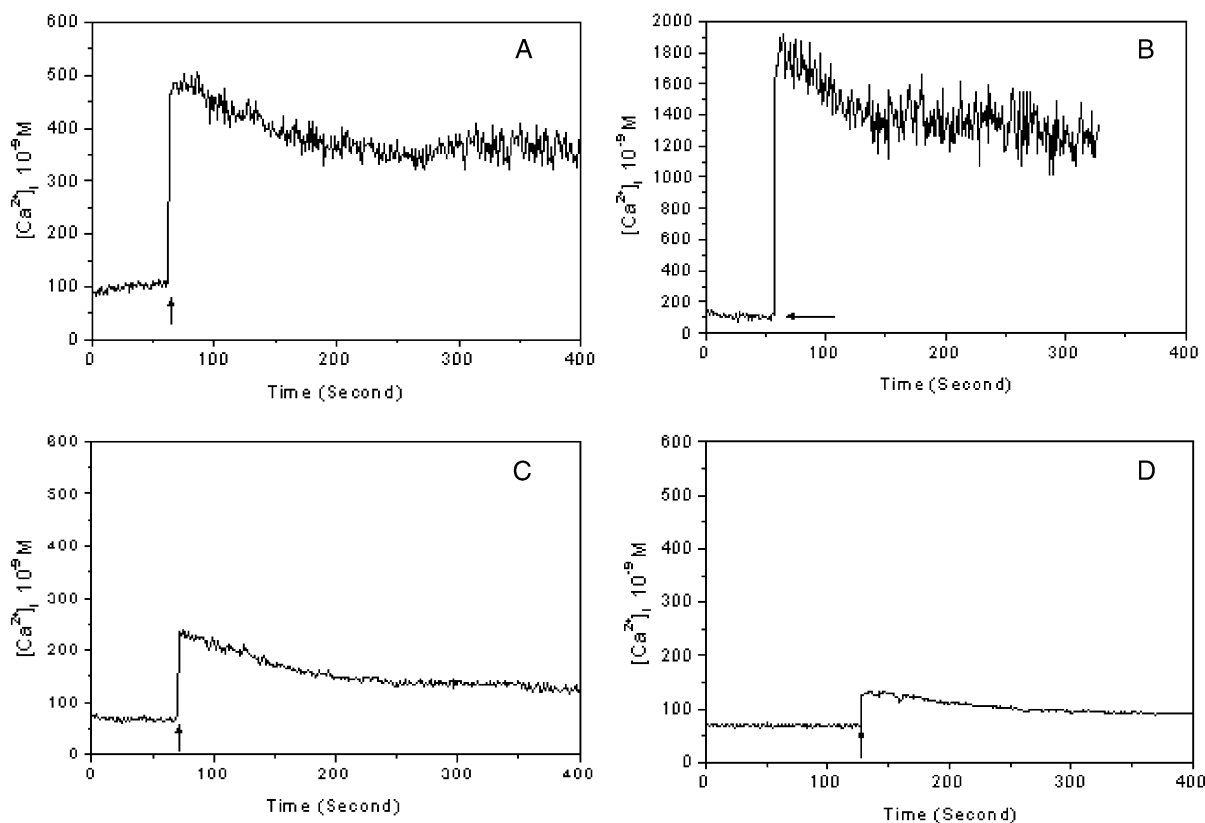


Fig. 1. Changes of intracellular calcium concentration induced by 2-BA-2-DMHA and red light in 2 μM Fura-2/Am-loaded MGC-803 cells. Cells (10^6 cells/ml) were treated with: (A) 4 μM , 12 J cm^{-2} ; (B) 8 μM , 12 J cm^{-2} ; (C) 4 μM , 1.5 J cm^{-2} 2-BA-2-DMHA and light dose in Krebs solution; and (D) 4 μM , 3 J cm^{-2} 2-BA-2-DMHA and light dose in Ca^{2+} -free Krebs solution. The light dose was added at the time point indicated by the arrow. Experiments were carried out at 37 °C on a dual excitation fluorescence spectrophotometer.

fluorescence microscope (NIKON Inverted Microscope DIAPHOT 300) equipped with aquacosmos software (HAMAMATSU, Japan), using 340 nm excitation and a 450 nm barrier.

All data were expressed as mean \pm S.D. (standard deviation); for comparisons of the means, we used Student's *t*-test. *P*-values less than 0.05 are considered statistically significant.

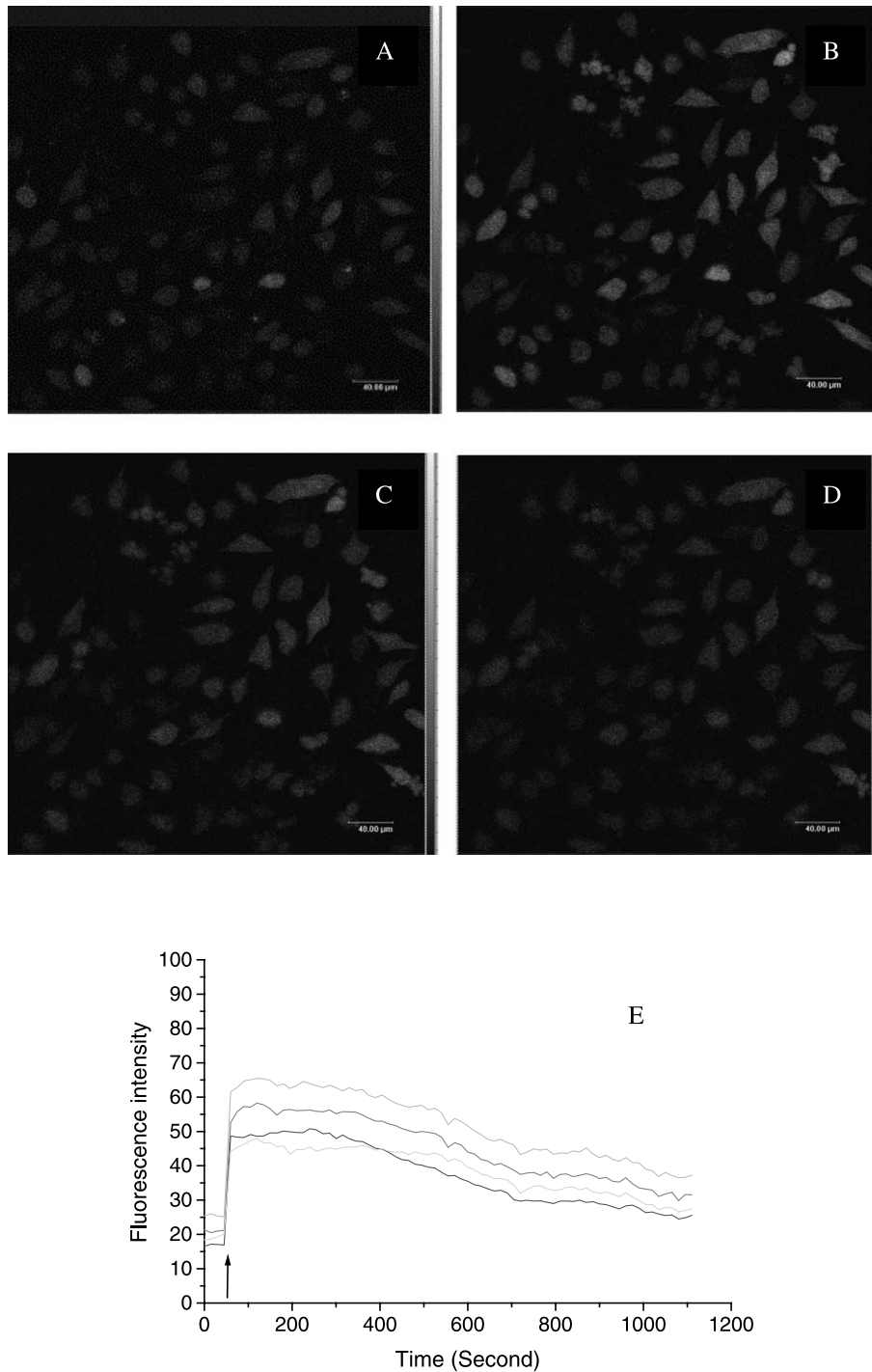


Fig. 2. Confocal images and the fluorescence intensity of intracellular calcium signal in MGC-803 cells induced by 2-BA-2-DMHA and 3 J cm^{-2} of light dose in the presence of extracellular Ca^{2+} . The cells, in monolayer, were incubated with $8 \mu\text{M}$ 2-BA-2-DMHA for 4 h, then washed and loaded with $10 \mu\text{g ml}^{-1}$ Fluo-3/Am for another 30 min. Measurements were taken at 37°C on a laser scanning confocal microscope: (A) 0 s; (B) immediately; (C) 250 s; (D) 1050 s after PDT; (E) the changes of fluorescence intensity in four cells as a function of time.

3. Results

3.1. Changes in intracellular Ca^{2+} concentration related to PDT

The membrane-permeable Fura-2/AM is hydrolyzed by the endogenous acetoxymethyl esterase to form Fura-2,

which is characterized by low fluorescence. Fura-2 specifically binds to intracellular free Ca^{2+} and the Fura-2- Ca^{2+} complex shows strong fluorescence [25]. The excitation wavelength of Fura-2 and the Fura-2- Ca^{2+} complex are 380 and 340 nm, respectively. We measured intracellular free Ca^{2+} by fluorescence spectroscopy using dual-exciting wavelengths [26]. Fig. 1 showed the changes in $[Ca^{2+}]_i$ as a

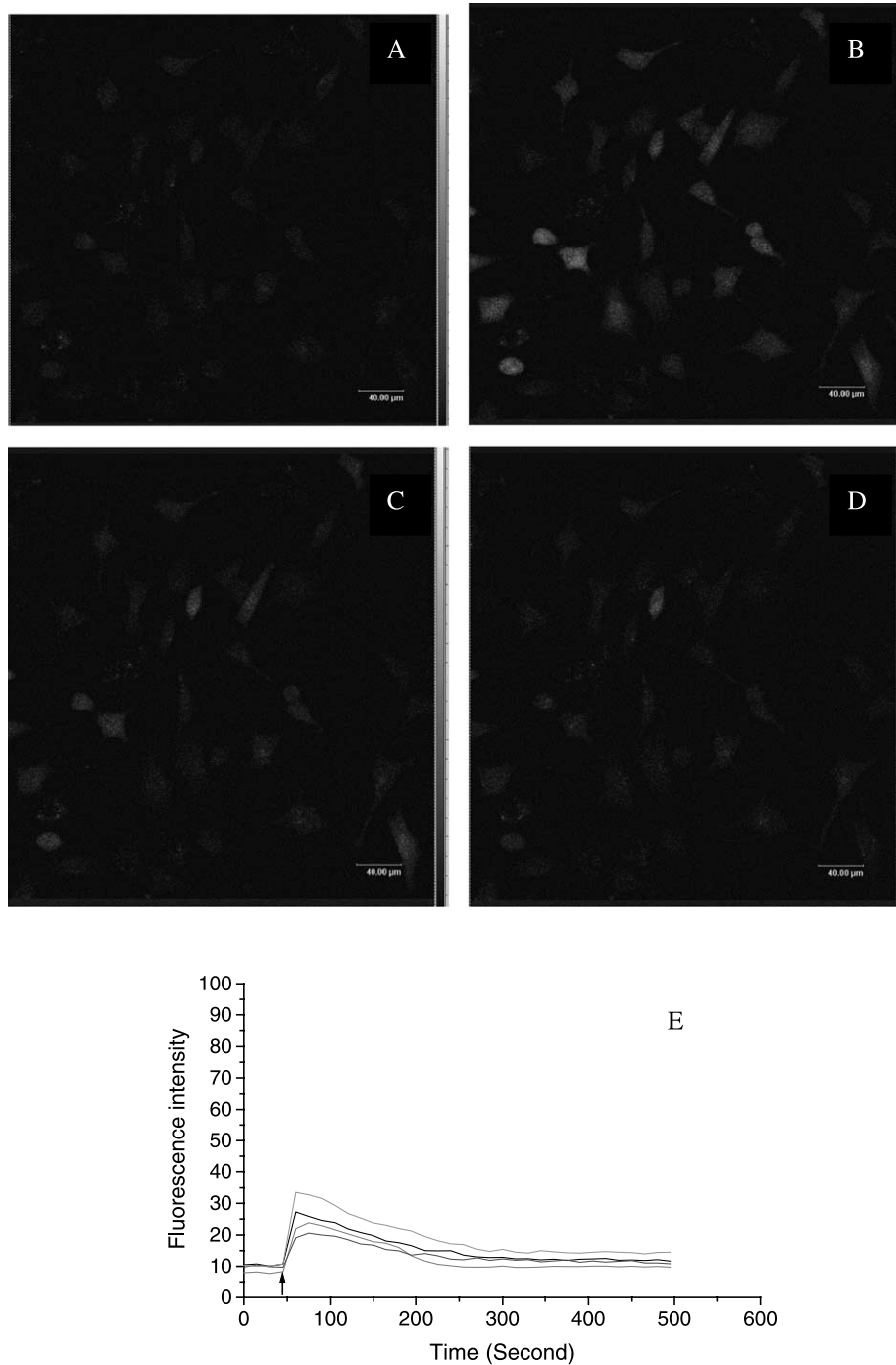


Fig. 3. Confocal images and the fluorescence intensity of intracellular calcium signal in MGC-803 cells induced by 2-BA-2-DMHA and 3 J cm^{-2} of light dose in the absence of extracellular Ca^{2+} . The cells, in monolayer, were incubated with $8 \mu\text{M}$ 2-BA-2-DMHA for 4 h, then washed and loaded with $10 \mu\text{g ml}^{-1}$ Fluo-3/Am for another 30 min. Measurements were taken at 37°C on a laser scanning confocal microscope: (A) 0 s; (B) immediately; (C) 100 s; (D) 300 s after PDT; (E) the changes of fluorescence intensity in four cells as a function of time.

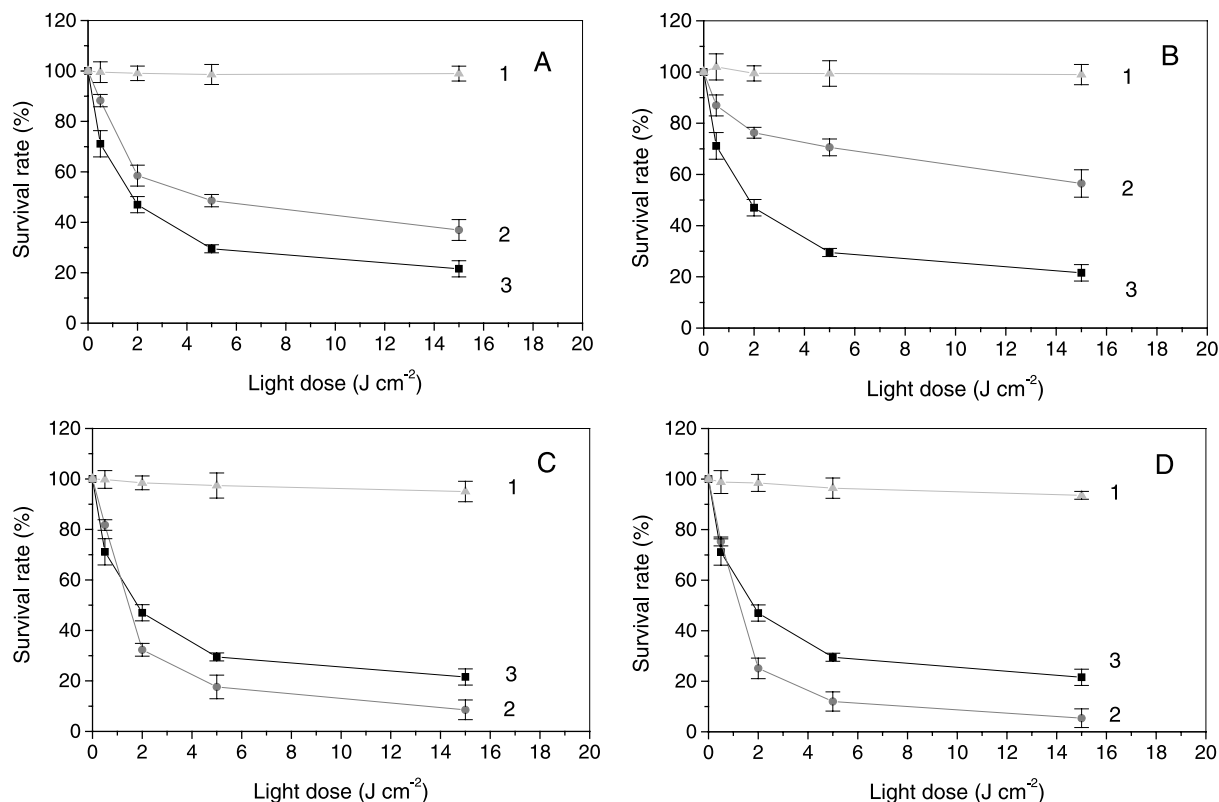


Fig. 4. Effects of EGTA, BAPTA, TG and A23187 on phototoxicity of 2-BA-2-DMHA to MGC-803 cells. (A): (1) 0.5 mM EGTA, 0 μM 2-BA-2-DMHA; (2) 0.5 mM EGTA, 8 μM 2-BA-2-DMHA; (3) 0 mM EGTA, 8 μM 2-BA-2-DMHA; (B): (1) 3 μM BAPTA, 0 μM 2-BA-2-DMHA; (2) 3 μM BAPTA, 8 μM 2-BA-2-DMHA; (3) 0 μM BAPTA, 8 μM 2-BA-2-DMHA; (C): (1) 3 μM TG, 0 μM 2-BA-2-DMHA; (2) 3 μM TG, 8 μM 2-BA-2-DMHA; (3) 0 μM TG, 8 μM 2-BA-2-DMHA; (D): (1) 3 μM A23187, 0 μM 2-BA-2-DMHA; (2) 3 μM A23187, 8 μM 2-BA-2-DMHA; (3) 0 μM A23187, 8 μM 2-BA-2-DMHA. Representative results were shown as the mean \pm S.D. from two independent experiments.

function of time before and after 2-BA-2-DMHA-PDT in MGC-803 cells. Evidently, there was a rapid increase in $[Ca^{2+}]_i$ from the basal level immediately after red light exposure, reaching a peak. Then, $[Ca^{2+}]_i$ declined; however, it did not return to the resting level but attained a new steady state with a higher $[Ca^{2+}]_i$ level.

At physiological $[Ca^{2+}]_e$ (10^{-3} M), the average $[Ca^{2+}]_i$ of MGC-803 cells measured in this experiment was 90 ± 30 nM. Irradiation of MGC-803 cells incubated with sensitizer led to increases of the $[Ca^{2+}]_i$ that depended upon both the concentration of 2-BA-2-DMHA and light fluence. As shown in Fig. 1A,B, at 12 J cm^{-2} fluence, increasing the concentration of 2-BA-2-DMHA from 4×10^{-6} to 8×10^{-6} M increased the peak calcium increase about 2.6-fold (= maximum). And also with the same concentration of (8×10^{-6} M), the magnitude of $[Ca^{2+}]_i$ increased 1-fold (= maximum) after irradiation with 1.5 and 12 J cm^{-2} , respectively (Fig. 1C,A).

To determine whether influx of external Ca^{2+} was the source of elevated $[Ca^{2+}]_i$ after 2-BA-2-DMHA-PDT, cells treated with the same concentration of photosensitizer were given irradiation in Krebs solution and Ca^{2+} -free Krebs solution, respectively. As shown in Fig. 1D, when cells were irradiated with 3 J cm^{-2} of light dose in the absence of

$[Ca^{2+}]_e$, there was a much smaller increase in $[Ca^{2+}]_i$ than that in the presence of physiological $[Ca^{2+}]_e$ (Fig. 1C, with 1.5 J cm^{-2}). It suggested that the rise in $[Ca^{2+}]_i$ was greatly due to the influx of Ca^{2+} from the extracellular medium.

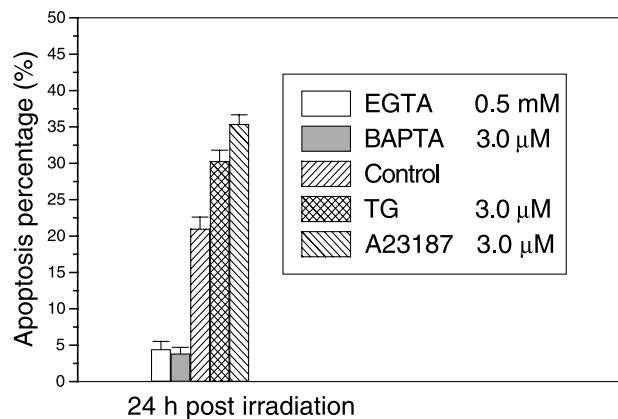


Fig. 5. Effects of EGTA, BAPTA, TG and A23187 on the percentages of apoptotic MGC-803 cells after PDT with $8 \mu\text{M}$ 2-BA-2-DMHA and 5 J cm^{-2} light dose. The experiments were carried out at 37°C on a flow cytometry. Representative results were shown as the mean \pm S.D. from two independent experiments (significantly different from control sample, $P < 0.05$, compared with control sample according to Student's *t*-test).

The small increase of $[Ca^{2+}]_i$ after PDT in the absence of extracellular Ca^{2+} medium might derive from intracellular calcium store such as the endoplasmic reticulum, mitochondria, the nucleus or other calcium-storing cell organelles or calcium-binding proteins [27,28].

3.2. Visualization of changed in $[Ca^{2+}]_i$ with LSCM

Recently, changes in $[Ca^{2+}]_i$ have been measured by confocal laser microscopy using Fluo-3 as an indicator [13,29]. In the present study, we adopted the procedure to

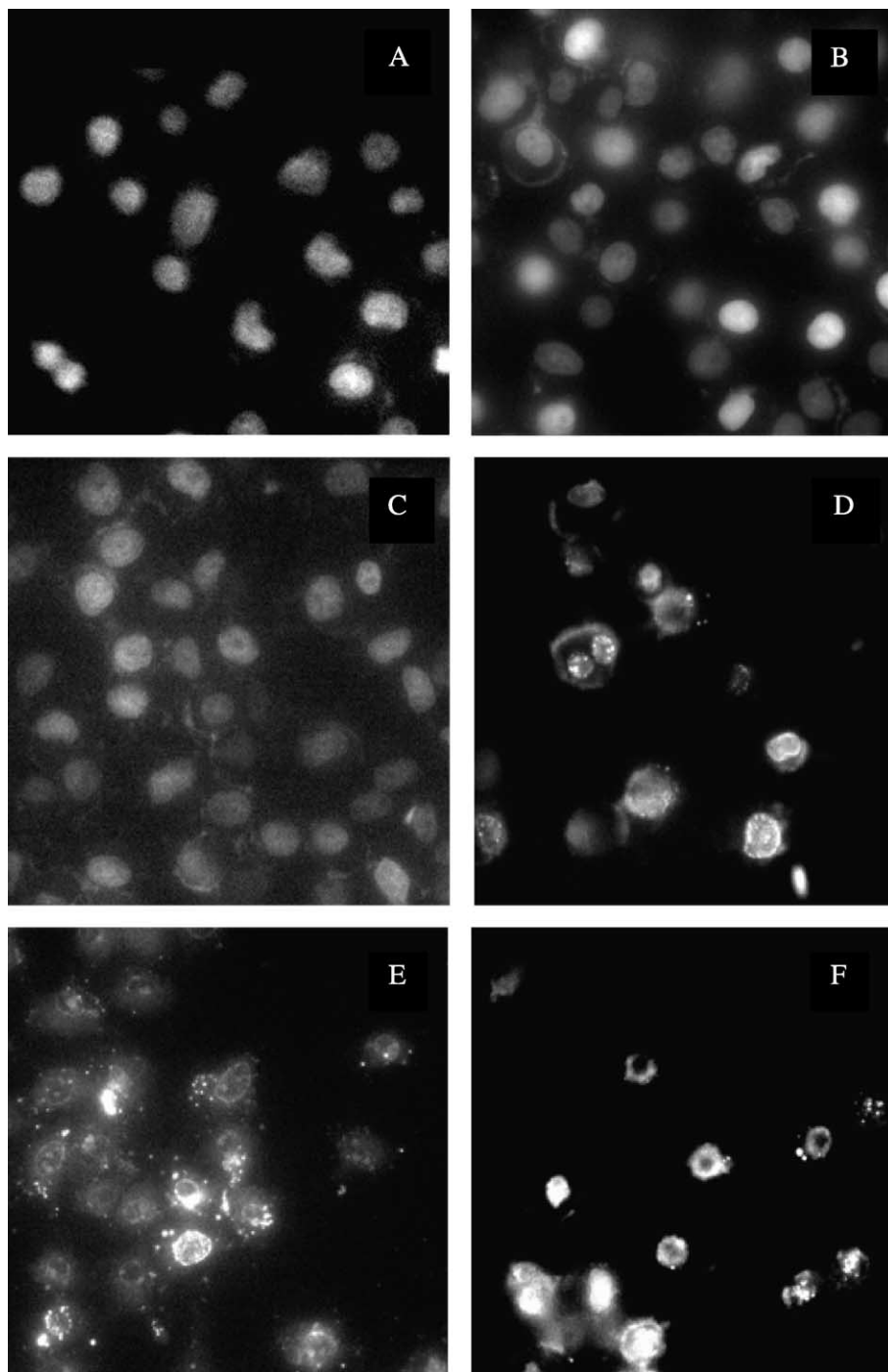


Fig. 6. Effects of EGTA, BAPTA, TG and A23187 on the nuclear morphology of MGC-803 cells after PDT with 2-BA-2-DMHA and 8 J cm^{-2} light dose. Cells were incubated with $8 \mu\text{M}$ 2-BA-2-DMHA for 4 h and treated with 0.5 mM EGTA (A); $3 \mu\text{M}$ BAPTA (B); $3 \mu\text{M}$ TG (E) and $3 \mu\text{M}$ A23187 (F), then irradiated with 8 J cm^{-2} of light dose. After 20 h, cells were incubated with Hoechst 33258, and nuclear morphology was investigated on a fluorescence microscope; (C) untreated control cells ($0 \mu\text{M}$ 2-BA-2-DMHA and 0 J cm^{-2} of light dose); (D) only treated with $8 \mu\text{M}$ 2-BA-2-DMHA and 8 J cm^{-2} of light dose.

detect the fluorescence signals arising from the individual MGC-803 cells loaded with Fluo-3/Am. Two-dimensional (2-D) confocal images showed that 2-BA-2-DMHA-PDT elicited a rapid and transient increase in the $[Ca^{2+}]_i$, measured as fluorescence intensity, of adherent MGC-803 cells both in Krebs solution (Fig. 2A–E) and Ca^{2+} -free Krebs solution (Fig. 3A–E). Fluorescence intensity was relatively low at the baseline (0 s, Figs. 2A and 3A), reached a peak immediately after PDT (Figs. 2B and 3B) and then declined (250 s, Fig. 2C; and 100 s, Fig. 3C) to a new lowest level (1050 s, Fig. 2D; and 300 s, Fig. 3D). As illustrated in the graphs in Figs. 2E and 3E, there was an intracellular calcium variability during PDT. However, this variability was more pronounced and prolonged among the cells in Krebs solution (Fig. 2E) than those in Ca^{2+} -free Krebs solution (Fig. 3E). It was also noticed that in the presence of extracellular calcium, after the rise elicited by PDT, the intracellular Ca^{2+} declined to a level (at 1050 s) which was obviously higher than the initial baseline level, while the intracellular Ca^{2+} declined to a level (at 300 s) which was slightly higher than the initial one in the absence of extracellular Ca^{2+} . CLSM results suggested the increased intracellular Ca^{2+} after PDT was mainly from the influx of extracellular Ca^{2+} .

The results from LSCM further supported the observations presented in Fig. 1.

3.3. Effects of $[Ca^{2+}]_i$ changes on the MGC-803 cells survival

It is reported that cytotoxicity induced by various xenobiotics appears to involve elevated $[Ca^{2+}]_i$ in many cases [2,6,7,10]. Thus, in order to investigate whether the increase in $[Ca^{2+}]_i$ after 2-BA-2-DMHA-PDT was involved in phototoxicity, the cells were loaded with extracellular calcium chelator EGTA, intracellular calcium chelator BAPTA, inhibitor of the ER-associated Ca^{2+} pump TG, and a calcium ionophore Br-A23187 prior to light exposure, respectively, and then the MTT assay was performed.

Survival curves of the phototoxicity of 2-BA-2-DMHA in different calcium level conditions were shown in Fig. 4A–D. The results showed that the survival of cells after PDT depended on both $[Ca^{2+}]_i$ and $[Ca^{2+}]_e$, that is, a decrease of the $[Ca^{2+}]_e$ by EGTA or $[Ca^{2+}]_i$ by BAPTA during PDT was in favor of the cell survival (Fig. 4A,B), whereas an increase of $[Ca^{2+}]_i$ by TG or Br-A23187 could enhance the cell killing of 2-BA-2-DMHA-PDT (Fig. 4C,D).

3.4. Involvement of intracellular Ca^{2+} in 2-BA-2-DMHA photoinduced cell apoptosis

To test whether intracellular Ca^{2+} acted as a mediator in 2-BA-2-DMHA photoinduced MGC-803 cell apoptosis, we examined the effects of EGTA, BAPTA, TG and A23187 on the PDT-induced cell apoptosis. Quantitative analysis of apoptosis was performed by flow cytometry by staining nuclear with PI and determining hypodiploid DNA content

[30]. The percentages of apoptosis MGC-803 along with incubation time post-irradiation were shown in Fig. 5. The results suggested that treatment with EGTA and BAPTA significantly suppressed, while TG and A23187 enhanced the 2-BA-2-DMHA photoinduced apoptosis in MGC-803 cells. That is, an increase of intracellular Ca^{2+} may play an important positive role in 2-BA-2-DMHA photoinduced apoptosis in MGC-803 cells.

3.5. Identification of apoptotic nucleus by Hoechst 33258 staining

Results from a fluorescence microscope (NIKON Inverted Microscope DIAPHOT 300) equipped with aquacosmos software further supported the observations presented above. EGTA, BAPTA, TG, A23187 were used to change the concentration of extracellular and intracellular calcium during 2-BA-2-DMHA-PDT, and the nuclear morphology of dying cells were investigated using the nuclear staining Hoechst 33258. As shown in Fig. 6A–F, 20 h after being treated with 8 μ M 2-BA-2-DMHA and 8 J cm^{-2} of light dose, there was less chromatin concentration in EGTA (Fig. 6A) or BAPTA (Fig. 6B) treated cells than in control cells (Fig. 6D). In contrast, a typical apoptotic nucleus presented in TG- (Fig. 6E) and A23187- (Fig. 6F) treated samples had more nuclear condensation.

The effects of EGTA, BAPTA, TG and A23187 on the concentrations of extracellular and intracellular calcium and the percentage of apoptosis induced by PDT suggested that the increase of intracellular Ca^{2+} might be necessary and specific to photoinduced damage of 2-BA-2-DMHA to MGC-803 cells.

4. Discussion

To better understand the phototoxicity of 2-BA-2-DMHA to MGC-803 cells, we investigated the concentration changes of intracellular calcium and the relationship between cell damage and the increase of $[Ca^{2+}]_i$.

After photosensitization of MGC-803 cells by 2-BA-2-DMHA, a transient increase of $[Ca^{2+}]_i$ was observed. As shown in Fig. 1, at physiological $[Ca^{2+}]_e$, PDT was accompanied by an increase of $[Ca^{2+}]_i$ from mean basal level of 90 ± 30 nM to a maximum of more than 1800 nM immediately after the end of red light irradiation. This finding was in accordance with a number of reports in which a rise of $[Ca^{2+}]_i$ from resting level to the micromolar range after irradiation was found [31]. The results from the experiment with or without extracellular calcium suggested that the rise of $[Ca^{2+}]_i$ in the presence of physiological $[Ca^{2+}]_e$ appeared to be mainly due to the influx of extracellular Ca^{2+} (Fig. 1D, and Figs. 2 and 3), because the increase in $[Ca^{2+}]_i$ after 2-BA-2-DMHA-PDT was very small when Ca^{2+} influx was prevented by the absence of extracellular Ca^{2+} . The same results were also reported by Joshi et al., [11] Tarr et al. [31],

and Ver Donk et al. [32]. The results from Figs. 1–3 showed that the increases of $[Ca^{2+}]_i$ were concentration of 2-BA-2-DMHA-, light dose- and extracellular $[Ca^{2+}]_e$ -dependent.

Because all cells are bathed in a culture medium very rich in Ca^{2+} (10^{-3} M), while intracellular Ca^{2+} concentrations are much lower, on the order of 10^{-7} – 10^{-6} M [4–6]. The electrical potential across the plasma membrane of the cells tends to drive Ca^{2+} into them. Such a large electrochemical gradient is maintained by the relative impermeability of the plasma membrane to Ca^{2+} and by active extrusion. Damage to the plasma membrane by any one of a number of different mechanisms will disrupt this permeability barrier with a consequent influx of Ca^{2+} . Decrease in $[Ca^{2+}]_i$ with increasing post-irradiation time (as shown in Figs. 1–3) were mostly due to the plasma membrane partially recovered from photodynamic injury, Ca^{2+} extrusion into the external space, and/or re-sequestration into the calciosomes by the action of the Ca^{2+} pump which maintained Ca^{2+} homeostasis in the cell [33]. The mechanism by which Ca^{2+} may enter cells during PDT and how to try to recover the Ca^{2+} homeostasis in cells after PDT are currently under further investigation.

It was also noteworthy that in all the experiments with or without extracellular Ca^{2+} , although the Ca^{2+} response was transient, $[Ca^{2+}]_i$ levels did not return to the basal levels, but obtained a new steady state with higher $[Ca^{2+}]_i$ levels. It was likely that some of the Ca^{2+} buffering systems such as Ca^{2+} -ATPase, Na/Ca^{2+} exchange and intracellular stores such as endoplasmic reticulum, mitochondria, and even nuclear morphology were also affected by photosensitization, which in turn altered the cellular Ca^{2+} homeostasis leading to the new steady state. The abnormally higher $[Ca^{2+}]_i$ levels is, of course, not in favor of the survivals of cells. Calcium in the post-irradiation steady state was dependent on the concentration of 2-BA-2-DMHA, the light dose and the extracellular Ca^{2+} concentration.

$[Ca^{2+}]_i$ is a second messenger that regulates a large number of physiological processes in animal cell, for example, it can be a key signal leading to cell death, particularly when intracellular calcium concentration becomes abnormally high [1–4,6,7]. The role of elevated levels of $[Ca^{2+}]_i$ in a variety of pathological and toxicological processes were reported [10,12,34,35]. The present experiments showed that loading the cells with the exogenous calcium chelator, EGTA, and the endogenous calcium chelator BAPTA prior to PDT protected against cell killing, while TG, a highly specific inhibitor of the ER-associated Ca^{2+} pump, and Br-A23187, a calcium ionophore enhanced the killing (Figs. 4–6). This is the evidence that the elevation of $[Ca^{2+}]_i$ is involved in the pathological processes leading to cell death. EGTA, BAPTA, TG and A23187 were only present during irradiation and a short period thereafter, until the mediums were replaced by culture medium. The results of control experiments showed that the effect on survival could only have occurred during the period when the calcium modulators were present. Our observation of cell toxicity following photosensitization

dependent on intracellular Ca^{2+} is similar to reports of mouse myeloma cells, murine L929 fibroblasts H9c2 cardiac cells, and cardiomyocytes [10,12,34,35]. However, it differs from the protective effects of Ca^{2+} in Chinese hamster ovary cells, T24 human bladder transitional carcinoma cells and human skin fibroblasts [7,36], where some authors have connected transient increases in intracellular Ca^{2+} concentration with protection against phototoxicity [37]. In MGC-803 cells, it is clear that intracellular Ca^{2+} contributes to the observed phototoxicity. This dichotomy is evident following different cell types and different photosensitizers. In some cell types, mild photosensitized modification leads to a transient increase in intracellular calcium concentration, and this may be associated with a protective response allowing the cell to survive in the insult [36]. In other cell types, or with stronger photosensitization conditions, the increase in intracellular calcium concentration is sharp and prolonged. The sustained elevation of $[Ca^{2+}]_i$ has a number of deleterious effects including activation of phospholipases, proteases, endonucleases [38]. Endonuclease activation results in single and double DNA strand breaks, which in turn, stimulate increased levels of p53. Activation of proteases modifies a number of substrates including actin and related proteins leading to bleb formation. Phospholipase activation modifies membrane permeability. Increase of $[Ca^{2+}]_i$ is also associated with activation of a number of protein kinases such as MAP kinase, calmodulin kinase. Such kinases are involved in activation of transcription factors, which initiate transcription of immediate-early stress genes such as p53, following DNA strand breaks may induce cell death.

5. Conclusion

A transient increase of intracellular calcium level was observed in 2-BA-2-DMHA-PDT-treated MGC-803 cells, and the calcium influx played a major role in producing such an increase of intracellular calcium. The initial spurt in $[Ca^{2+}]_i$ and the persistently elevated $[Ca^{2+}]_i$ levels were dependent upon the concentration of 2-BA-2-DMHA, the light dose and the extracellular $[Ca^{2+}]_e$, and might activate a variety of cellular processes. It suggested that the abnormally high $[Ca^{2+}]_i$ was involved in the phototoxicity of 2-BA-2-DMHA to MGC-803 cells. But more work is still required to establish under what conditions cell death is triggered by an increased $[Ca^{2+}]_i$ following PDT and what is the signal transduction pathway for this process.

Acknowledgements

This work was supported by the National Natural Science Foundation of China (Grant No. 30070194) and the Special Group Foundation of the Chinese Academy of Sciences.

References

- [1] H. Rasmussen, The calcium messenger system, *N. Engl. J. Med.* 314 (1986) 1094–1101.
- [2] F.A.X. Schanne, A.B. Kane, E.E. Young, J.L. Farber, Calcium dependence of toxic cell death: a final common pathway, *Science* 206 (1979) 700–702.
- [3] D.J. McConkey, S. Orrenius, Breakthroughs and views: the role of calcium in the regulation of apoptosis, *Biochem. Biophys. Res. Commun.* 239 (1997) 357–366.
- [4] F. Antoine, J.E. Faure, C. Dumas, J.A. Feijo, Differential contribution of cytoplasmic Ca^{2+} and Ca^{2+} influx to gamete fusion and egg activation in maize, *Nat. Cell Biol.* 3 (2001) 1120–1123.
- [5] Cytoplasmic free calcium changes as a trigger mechanism in the response of cells to photosensitization, Yearly Review, *Photochem. Photobiol.* 58 (6) (1993) 890–894.
- [6] M. Dellinger, F. Ricchelli, G. Moreno, C. Salet, Hematoporphyrin derivative (Photofrin®) photodynamic action on Ca^{2+} transport in monkey kidney cells (CV-1), *Photochem. Photobiol.* 60 (4) (1994) 368–372.
- [7] A. Hubmer, A. Hermann, K. Uberriegler, B. Krammer, Role of calcium in photodynamically induced cell damage of human fibroblasts, *Photochem. Photobiol.* 64 (1) (1996) 211–215.
- [8] H. Rasmussen, The calcium messenger system, *N. Engl. J. Med.* 314 (1986) 1094–1101.
- [9] P. Nicotera, G. Bellomo, S. Orrenius, The role of Ca^{2+} in cell killing, *Chem. Res. Toxicol.* 3 (1990) 484–494.
- [10] K.G. Specht, M.A.J. Rodgers, Plasma membrane depolarization and calcium influx during cell injury by photodynamic action, *Biochim. Biophys. Acta* 1070 (1991) 60–68.
- [11] P.G. Joshi, K. Joshi, S. Mishra, N.B. Joshi, Ca^{2+} influx induced by photodynamic action in human cerebral glioma (U-87 MG) cells: possible involvement of a calcium channel, *Photochem. Photobiol.* 60 (3) (1994) 244–248.
- [12] L.C. Penning, J.W.M. Lagerberg, J.H. Van Dierendonck, C.J. Cornelisse, T.M.A.R. Dubbelman, J. Van Steveninck, The role of DNA and inhibition of poly (ADP-ribosyl)ation in loss of clonogenicity of murine L929 fibroblasts, caused by photodynamically induced oxidative stress, *Cancer Res.* 54 (1994) 5561–5567.
- [13] H. Tajiri, A. Hayakawa, Y. Matsumoto, I. Yokoyama, S. Yoshida, Changes in intracellular Ca^{2+} concentrations related to PDT-induced apoptosis in photosensitized human cancer cells, *Cancer Lett.* 128 (1998) 205–210.
- [14] D.P. Kelsen, Introduction: gastric cancer, *Sem. Surg. Oncol.* 23 (1996) 279–280.
- [15] M.L. Jin, B.Q. Wang, W. Zhang, Y.M. Wang, Photodynamic therapy for upper gastrointestinal tumors over the past 10 years, *Sem. Surg. Oncol.* 10 (1994) 111–113.
- [16] Y. Hayata, H. Kato, C. Konaka, J. Ono, M. Saito, H. Takahashi, T. Tomono, Photoradiation therapy in early stage cancer cases of the lung, esophagus and stomach, in: A. Andreoni, R. Cubeddu (Eds.), *Porphyryns in Tumor Therapy*, Plenum, New York, 1983, pp. 405–412.
- [17] W.G. Zhang, M. Weng, S.Z. Pang, M.H. Zhang, H.Y. Yong, H.X. Zhao, Z.Y. Zhang, A novel photosensitizer, 2-butylamino-2-demethoxy-hypocrellin A (2-BA-2-DMHA), 1. Synthesis of 2-BA-2-DMHA and its phototoxicity to MGC803 cells, *J. Photochem. Photobiol., B Biol.* 44 (1998) 21–28.
- [18] W.G. Zhang, L.P. Ma, S.W. Wang, H.Y. Yang, Z.Y. Zhang, Antisense Bcl-2 retrovirus vector increases the sensitivity of a human gastric adenocarcinoma cell line to photodynamic therapy, *Photochem. Photobiol.* 69 (5) (1999) 582–586.
- [19] H.Y. Yang, W.G. Zhang, L.P. Ma, S.W. Wang, Z.Y. Zhang, An approach to enhancing the phototoxicity of a novel hypocrellin congener to MGC803 cells, *Dyes Pigm.* 51 (2001) 103–110.
- [20] L. Beani, C. Tomasini, B.M. Govoni, C. Bianchi, Fluorimetric determination of electrically evoked increase in intracellular calcium in cultured cerebellar granule cells, *J. Neurosci. Methods* 51 (1994) 1–7.
- [21] A. Ciardo, J. Meldolesi, Regulation of intracellular calcium in cerebellar granule neurons: effects of depolarization and of glutamatergic and cholinergic stimulation, *J. Neurochem.* 56 (1991) 184–191.
- [22] G. Grynkiewicz, M. Poenie, R. Tsien, A new generation of Ca^{2+} indicators with greatly improved fluorescence properties, *J. Biol. Chem.* 260 (1985) 3440–3450.
- [23] A.M. Richter, E. Waterfield, A.K. Jain, E.D. Sternberg, D. Dolphin, J.G. Levy, In vitro evaluation of phototoxic properties of four structurally related benzoporphyrin derivatives, *Photochem. Photobiol.* 52 (1990) 495–500.
- [24] A.M.R. Fisher, K. Danenberg, D. Banerjee, J.R. Bertino, P. Danenberg, C.J. Gomer, Increased photosensitivity in HL60 cells expressing wild-type p53, *Photochem. Photobiol.* 66 (1997) 265–270.
- [25] R.A. Hirst, C. Harootunian, K. Hirota, Measurement of $[\text{Ca}^{2+}]_i$ in whole cell suspensions using Fura-2, *Methods Mol. Biol.* 114 (1999) 31–39.
- [26] A. Malgaroli, D. Milani, J. Meldolesi, T. Pozzan, Fura-2 measurement of cytosolic free Ca^{2+} in monolayers and suspensions of various types of animal cells, *J. Cell Biol.* 105 (1987) 2145–2155.
- [27] J. Meldolesi, P. Volpe, T. Pozzan, The intracellular distribution of calcium, *Trends Neurosci.* 11 (1988) 449–452.
- [28] A. Hermann, H.H. Kerschbaum, Immunocytochemical, biochemical and physiological characterization of calcium-binding proteins, in: J. Gu, G.W. Hacker (Eds.), *Modern Analytical Methods in Histology*, Plenum, New York, 1994, pp. 163–185.
- [29] X.J. Liang, Y.G. Huang, Intracellular free calcium concentration and cisplatin resistance in human lung adenocarcinoma A549 cells, *Biochem. Biophys. Res. Commun.* 273 (2000) 273–282.
- [30] W.G. Telford, L.E. King, P.J. Fraker, Rapid quantitation of apoptosis in pure and heterogeneous cell populations using flow cytometry, *J. Immunol. Methods* 172 (1994) 1–16.
- [31] M. Tarr, A. Frolov, D.P. Valzeno, Photosensitization-induced calcium overload in cardiac cell: direct link to membrane permeabilization and calcium influx, *Photochem. Photobiol.* 73 (4) (2001) 418–424.
- [32] L. Ver Donk, J. Van Reempts, G. Vandeplassche, M. Borgers, A new method to study activated oxygen species induced damage in cardiomyocytes and protection by Ca^{2+} -antagonists, *J. Mol. Cell. Cardiol.* J. Mol. Cell. Cardiol. 20 (1988) 811–823.
- [33] R. Anderson, A.G. Mahomed, Calcium efflux and influx in f-met-leu-phe (fMLP)-activated human neutrophils are chronologically distinct events, *Clin. Exp. Immunol.* 110 (1997) 132–138.
- [34] D.P. Valzeno, M. Tarr, Calcium as a modulator of photosensitized killing of H9c2 cardiac cells, *Photochem. Photobiol.* 74 (4) (2001) 605–610.
- [35] G. Yonuschot, Early increase in intracellular calcium during photodynamic permeabilization, *Free Radic. Biol. Med.* 11 (1991) 307–317.
- [36] L.C. Penning, M.H. Rasch, E. Ben-Hur, T.M.A.R. Dubbelman, A.C. Havelaar, J. Van Der Zee, J. Van Steveninck, A role for the transient increase of cytoplasmic free calcium in cell rescue after photodynamic treatment, *Biochim. Biophys. Acta* 1107 (1992) 255–260.
- [37] E. Ben-Hur, T.M.A.R. Dubbelman, Cytoplasmic free calcium changes as a trigger mechanism in the response of cells to photosensitization, *Photochem. Photobiol.* 58 (1993) 890–894.
- [38] B.F. Trump, Characteristics and mechanisms of cell injury and cell death: the role of $[\text{Ca}^{2+}]_i$, *Mar. Environ. Res.* 42 (1996) 57–63.